carbon number than the wax extracted from the catalyst. These results may indicate that the hydrocarbon product distribution may have shifted to higher carbon numbers toward the end of the run.

The Anderson-Schulz-Flory analysis for hydrocarbons resulted in $\alpha = 0.965$ in the C_{28}-C_{150} carbon number range (Figure 5-139).

After 212 hours of testing, Catalyst 4956-101 was reexamined, which revealed that the top portion of the catalyst bed was powdery, while the bottom portion was waxy. The powdery catalyst from the top portion did not have visible ruthenium particles according to the STEM examination. Also, the top portion showed very low ruthenium signal, suggesting that most of the ruthenium migrated to the bottom portion in the form of the ruthenium carbonyl. The bottom catalyst portion, on the other hand, showed 10-30 nm ruthenium particles, indicating that a substantial amount of agglomeration occurred with use of the catalyst. Since there was no noticeable amount of wax in the top catalyst portion, ruthenium migration from the top zone is believed to have occurred early in the run.

5.2.1.2.2 Test at 2.9 H_2:CO Feed Ratio, 208°C at Inlet and 11.2 atm

In an attempt to suppress ruthenium migration with $\leq$2-4 nm ruthenium particles, catalyst 4966-76 was tested at a low CO partial pressure in Run 19. The CO partial pressure was reduced relative to that in Run 17 both by increasing the H_2:CO feed ratio from 0.9 to 2.9 and by decreasing the total pressure from 35 to 11.2 atm. Other conditions were 208°C and 70 GHSV (Tables 5-26 and 5-27 and Figures 5-141 through 5-147).

Table 5-26. Product Distributions in Run 19

HEIGHT PCTS WITHOUT ARGON	
HYDROGEN	15.972
CARBON MONOXIDE	72.981
CARBON DIOXIDE	0.166
HATER	6.044
HYDROCARBONS	4.819
OXYGENATES	0.018
HYDROCARBON DISTRIBUTION	
C1	3.068
C2 - C4	4.310
C5 - C11	8.386
C12 - C18	13.899
C19 - C25	9.618
C26 PLUS	60.719
C1 - C44	58.511
C45 PLUS	41.489
OXYGENATES DISTRIBUTION	
ALCOHOLS	100.000
ALDEHYDES	0.000
OTHER OXYGENATES	0.000
HOLE PCTS WITHOUT ARGON	
HYDROGEN	72.724
CARBON MONOXIDE	23.917
CARBON DIOXIDE	0.035
HATER	3.079
HYDROCARBONS	0.240
OXYGENATES	0.004
RECOVERIES	
OVERALL	108.821
CARBON	108.348
HYDROGEN	108.971
OXYGEN	108.303
ARGON	108.851
CORRECTED RECOVERIES	
OVERALL	99.697
CARBON	99.538
HYDROGEN	100.110
OXYGEN	99.497

GAS ANALYSIS, HT%	
HYDROGEN	15.9719
CARBON MONOXIDE	72.9810
CARBON DIOXIDE	0.1661
METHANE	0.1478
ETHANE	0.0072
ETHYLENE	0.0134
PROPANE	0.0364
PROPYLENE	0.0522
BUTANE	0.0440
BUTENE	0.0544
AQUEOUS ANALYSIS, HT%	
HATER	6.0436
ALCOHOLS	
C1	0.0060
C2	0.0120
C3	0.0000
C4	0.0000
C5	0.0000
C6	0.0000
C7	0.0000
C8	0.0000
C9	0.0000
C10	0.0000
ALDEHYDES	
C1	0.0000
C2	0.0000
C3	0.0000
C4	0.0000
C5	0.0000
C6	0.0000
C7	0.0000
C8	0.0000
C9	0.0000
C10	0.0000
OTHER OXYGENATES	
C1	0.0000
C2	0.0000
C3	0.0000
C4	0.0000
C5	0.0000
C6	0.0000
C7	0.0000
C8	0.0000
C9	0.0000
C10	0.0000

Table 5-27. Hydrocarbon Distributions in Run 19

C1	3.0877	C51	0.8381	C101	0.2729	C151	0.0529	C201	0.0121
C2	0.4277	C52	0.8255	C102	0.2633	C152	0.0512	C202	0.0118
C3	1.8383	C53	0.8126	C103	0.2541	C153	0.0496	C203	0.0116
C4	2.0438	C54	0.7993	C104	0.2451	C154	0.0481	C204	0.0114
C5	2.2823	C55	0.7852	C105	0.2363	C155	0.0465	C205	0.0111
C6	0.2994	C56	0.7801	C106	0.2279	C156	0.0451	C206	0.0109
C7	0.6442	C57	0.7657	C107	0.2197	C157	0.0437	C207	0.0107
C8	1.0028	C58	0.7514	C108	0.2118	C158	0.0423	C208	0.0105
C9	1.2789	C59	0.7375	C109	0.2043	C159	0.0409	C209	0.0103
C10	1.5667	C60	0.7243	C110	0.1970	C160	0.0397	C210	0.0101
C11	1.3114	C61	0.7111	C111	0.1900	C161	0.0384	C211	0.0099
C12	1.3535	C62	0.6999	C112	0.1832	C162	0.0372	C212	0.0071
C13	1.6772	C63	0.6788	C113	0.1767	C163	0.0361	C213	0.0070
C14	2.0724	C64	0.6699	C114	0.1704	C164	0.0350	C214	0.0069
C15	2.1722	C65	0.6617	C115	0.1644	C165	0.0339	C215	0.0068
C16	2.3251	C66	0.6540	C116	0.1586	C166	0.0329	C216	0.0067
C17	2.2556	C67	0.6466	C117	0.1530	C167	0.0319	C217	0.0066
C18	2.0433	C68	0.6390	C118	0.1476	C168	0.0310	C218	0.0065
C19	1.7768	C69	0.6320	C119	0.1425	C169	0.0295	C219	0.0064
C20	1.5426	C70	0.6236	C120	0.1375	C170	0.0287	C220	0.0063
C21	1.3521	C71	0.6260	C121	0.1328	C171	0.0278	C221	0.0062
C22	1.3638	C72	0.6162	C122	0.1283	C172	0.0270	C222	0.0062
C23	1.2096	C73	0.6057	C123	0.1240	C173	0.0263	C223	0.0061
C24	1.2280	C74	0.5946	C124	0.1198	C174	0.0256	C224	0.0060
C25	1.1447	C75	0.5831	C125	0.1159	C175	0.0249	C225	0.0059
C26	1.1045	C76	0.5711	C126	0.1121	C176	0.0242	C226	0.0059
C27	1.1038	C77	0.5588	C127	0.1085	C177	0.0236	C227	0.0058
C28	1.0988	C78	0.5463	C128	0.1051	C178	0.0230	C228	0.0057
C29	1.0709	C79	0.5336	C129	0.1018	C179	0.0224	C229	0.0057
C30	1.0814	C80	0.5209	C130	0.0987	C180	0.0218	C230	0.0056
C31	1.0251	C81	0.5024	C131	0.0956	C181	0.0213	C231	0.0056
C32	1.0136	C82	0.4897	C132	0.0928	C182	0.0208	C232	0.0055
C33	0.9829	C83	0.4772	C133	0.0900	C183	0.0203	C233	0.0054
C34	0.9763	C84	0.4647	C134	0.0873	C184	0.0199	C234	0.0054
C35	0.9718	C85	0.4524	C135	0.0848	C185	0.0194	C235	0.0053
C36	0.9910	C86	0.4401	C136	0.0823	C186	0.0190	C236	0.0053
C37	0.9461	C87	0.4280	C137	0.0799	C187	0.0186	C237	0.0052
C38	0.9380	C88	0.4160	C138	0.0776	C188	0.0182	C238	0.0052
C39	0.9351	C89	0.4038	C139	0.0753	C189	0.0178	C239	0.0051
C40	1.0392	C90	0.3920	C140	0.0731	C190	0.0174	C240	0.0051
C41	0.9618	C91	0.3803	C141	0.0710	C191	0.0171	C241	0.0050
C42	0.9774	C92	0.3688	C142	0.0689	C192	0.0167	C242	0.0050
C43	0.9927	C93	0.3579	C143	0.0669	C193	0.0164	C243	0.0049
C44	1.0196	C94	0.3466	C144	0.0657	C194	0.0161	C244	0.0049
C45	0.9002	C95	0.3354	C145	0.0637	C195	0.0158	C245	0.0048
C46	0.8876	C96	0.3245	C146	0.0618	C196	0.0155	C246	0.0047
C47	0.8752	C97	0.3137	C147	0.0599	C197	0.0152	C247	0.0047
C48	0.8628	C98	0.3031	C148	0.0581	C198	0.0150	C248	0.0046
C49	0.8517	C99	0.2928	C149	0.0563	C199	0.0126	C249	0.0046
C50	0.8506	C100	0.2827	C150	0.0546	C200	0.0123	C250	0.0045

Figure 5-141. Catalyst 4966-76 with <2-4 nm Ruthenium Particles: Conversions in Run 19 (H_2:CO Feed Ratio = 2.9, 208°C at Inlet, 11.2 atm)

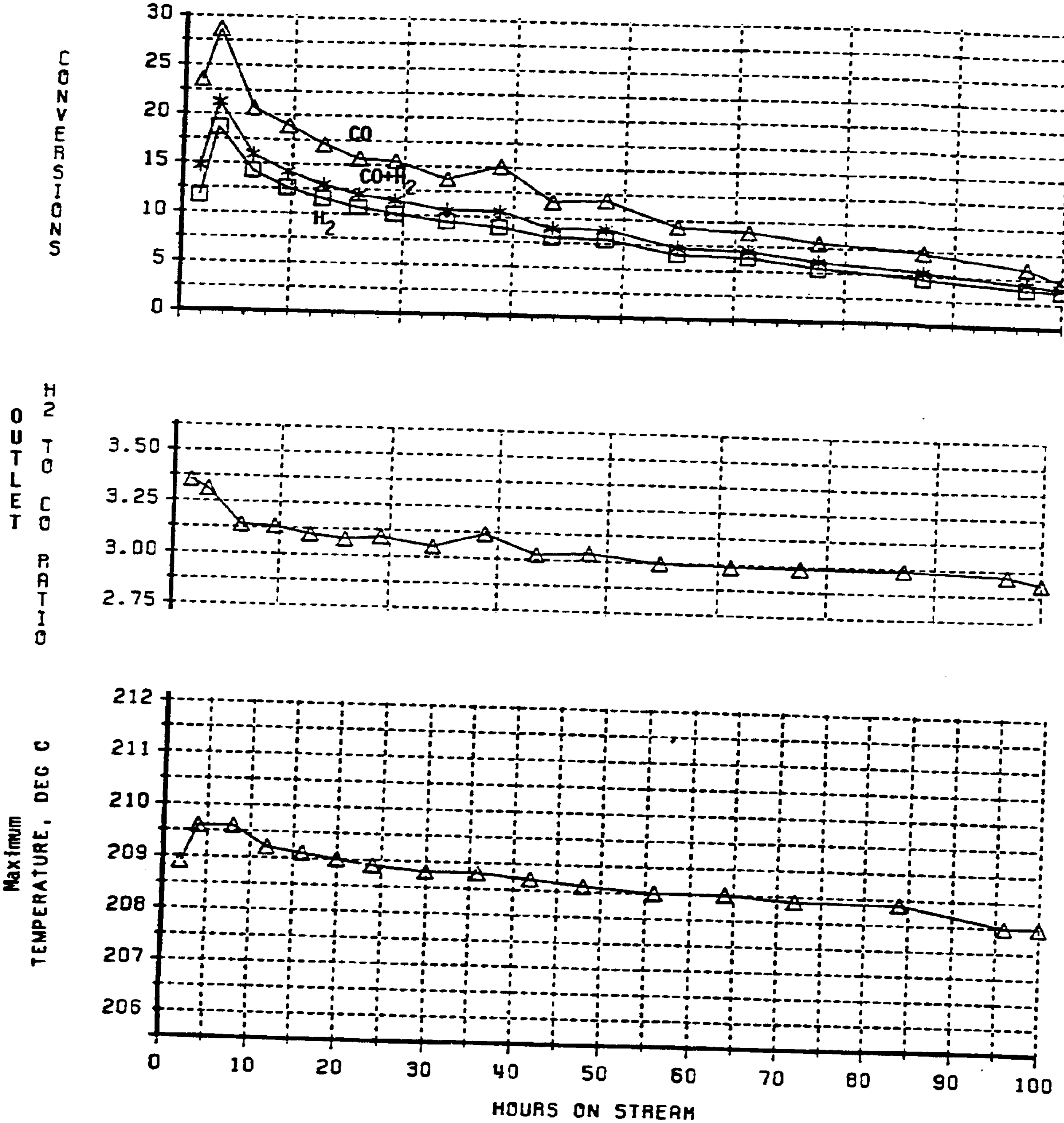

Figure 5-142. Catalyst 4966-76 with <2-4 nm Ruthenium Particles: Water Gas Shift Activity in Run 19 (H_2:CO Feed Ratio = 2.9, 208°C at Inlet, 11.2 atm)

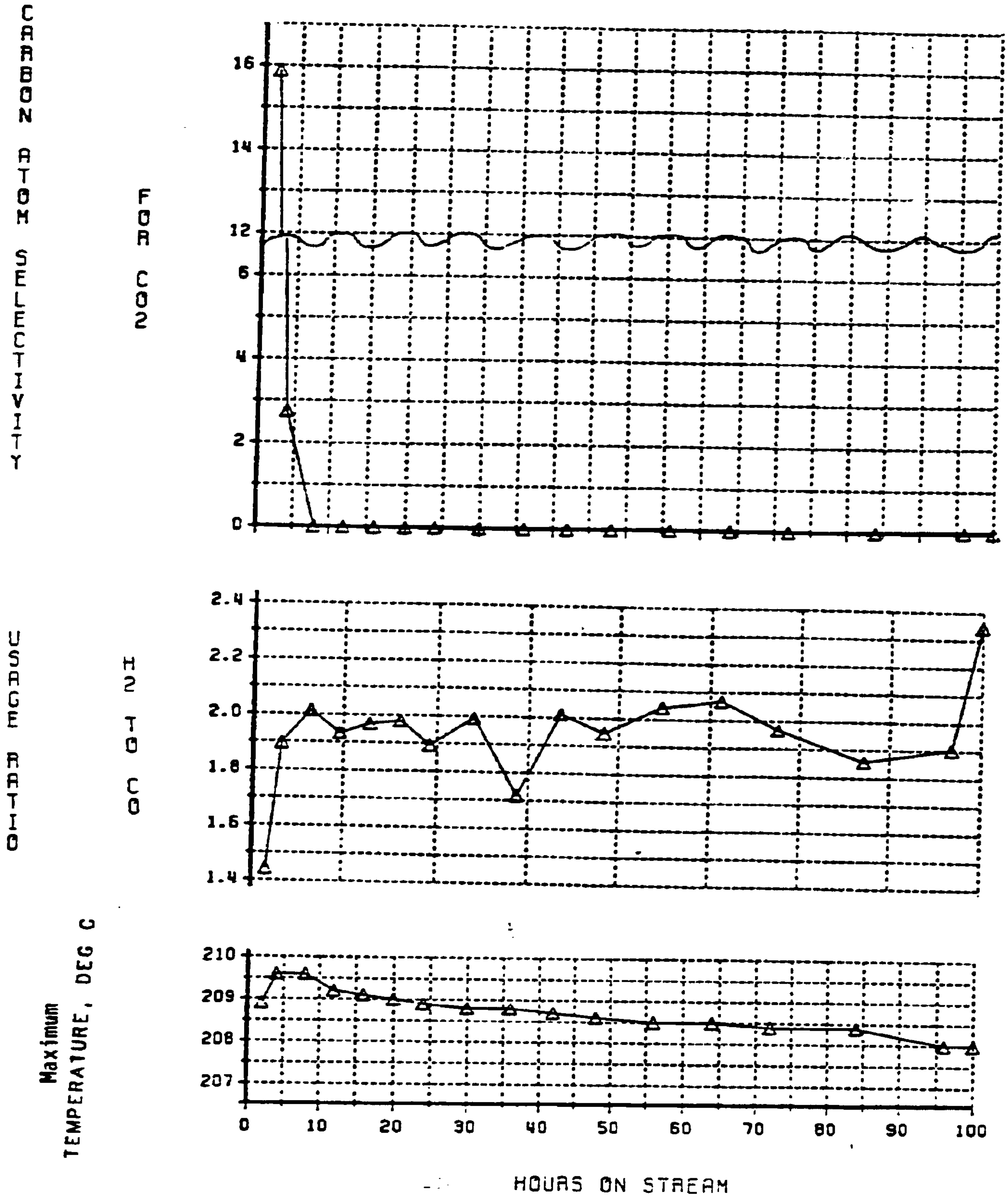

Figure 5-143. Catalyst 4966-76 with <2-4 nm Ruthenium Particles: C_1 and C_2 Selectivities in Run 19 (H_2:CO Feed Ratio = 2.9, 208°C at Inlet, 11.2 atm)

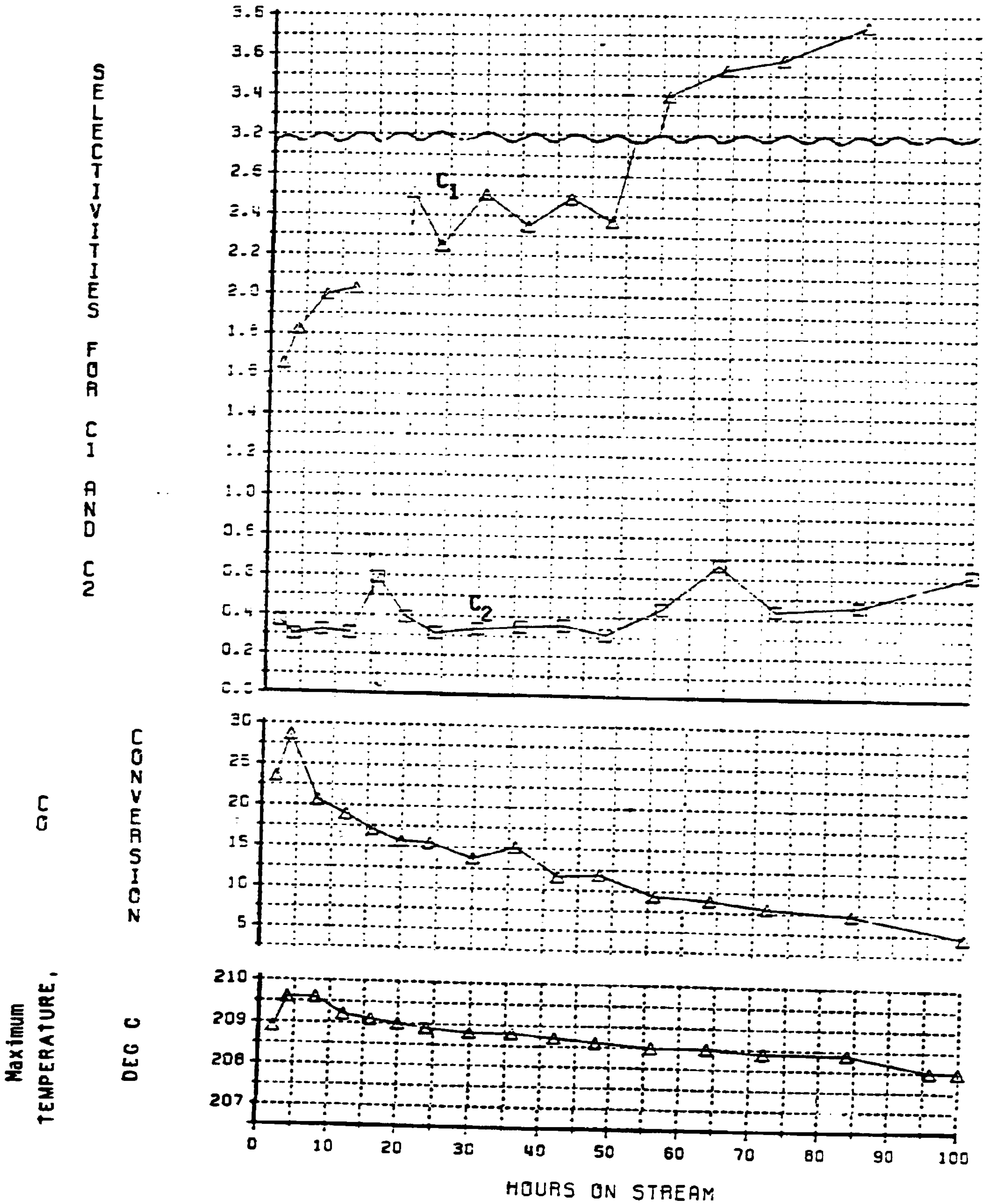

Figure 5-144. Catalyst 4966-76 with ≤2-4 nm Ruthenium Particles: C_3 and C_4 Selectivities in Run 19 (H_2:CO Feed Ratio = 2.9, 208°C at Inlet, 11.2 atm)

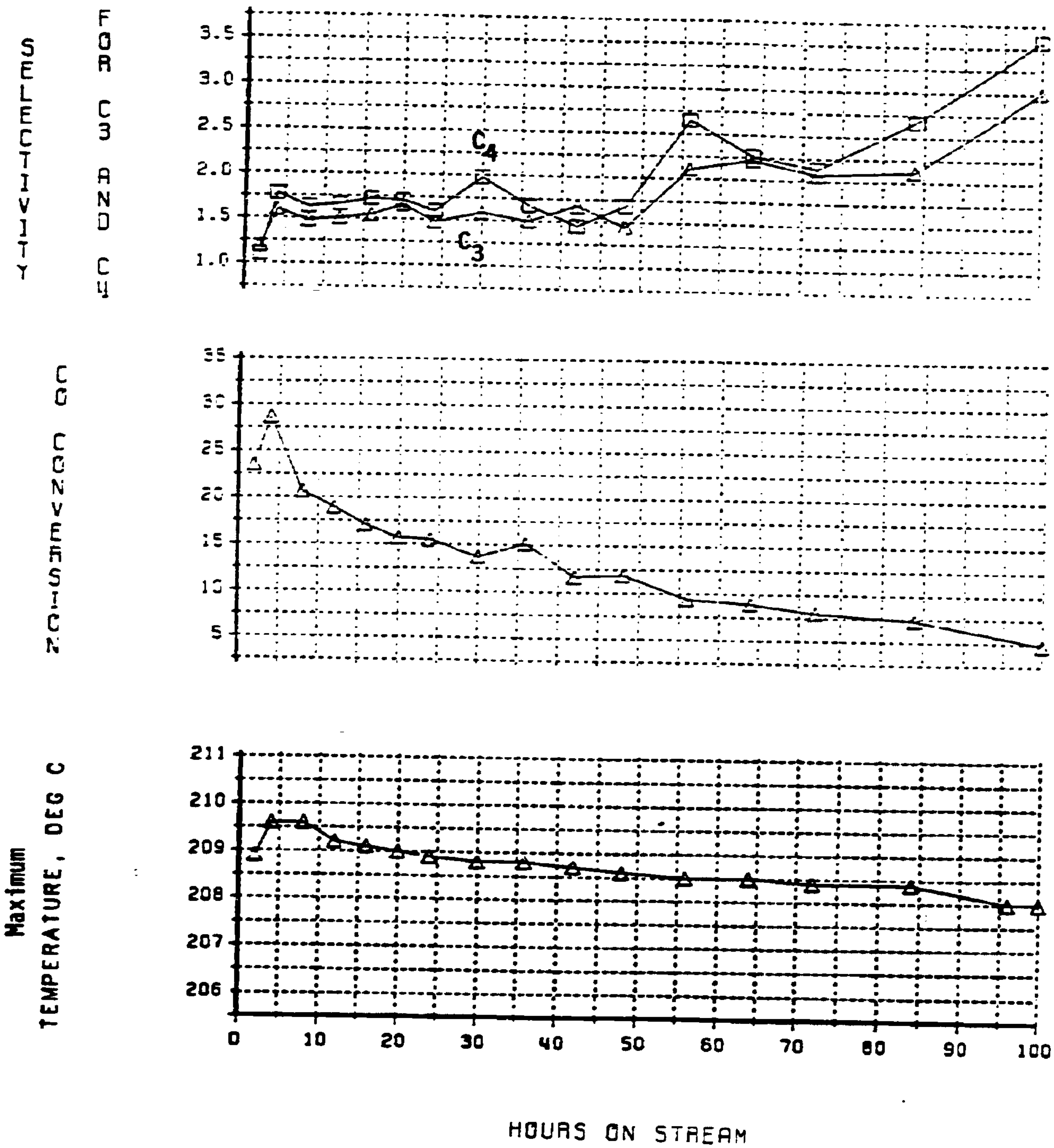

Figure 5-145. Catalyst 4966-76 with <2-4 nm Ruthenium Particles: Olefin to Paraffin Ratios in Run I9 (H_2:CO Feed Ratio = 2.9, 208°C at Inlet, 11.2 atm)

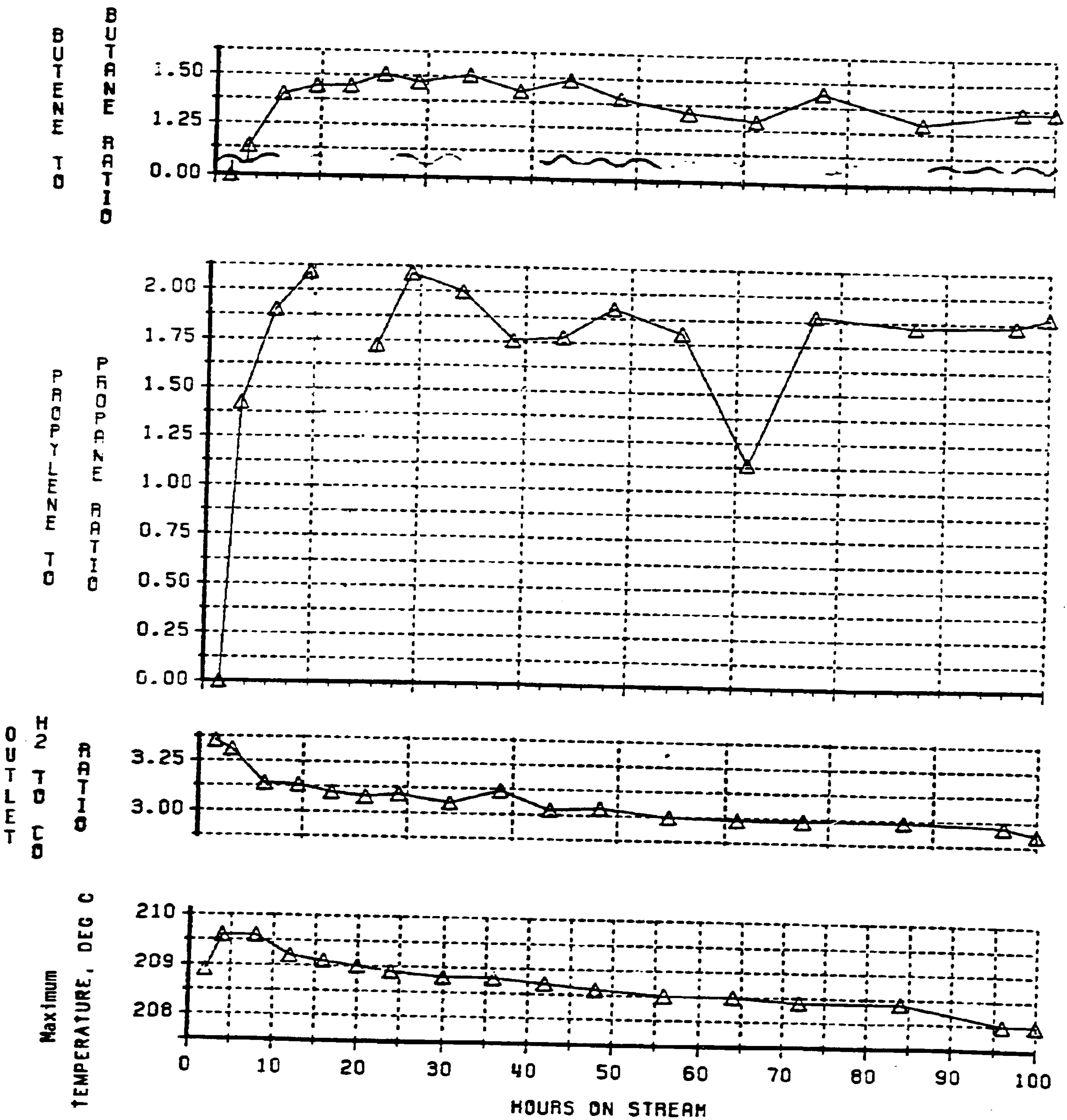

Figure 5-146. Anderson-Schulz-Flory Distributions with Catalyst 4966-76 with ≤2-4 nm Ruthenium in Run 19 (Hydrocarbons + Oxygenates)

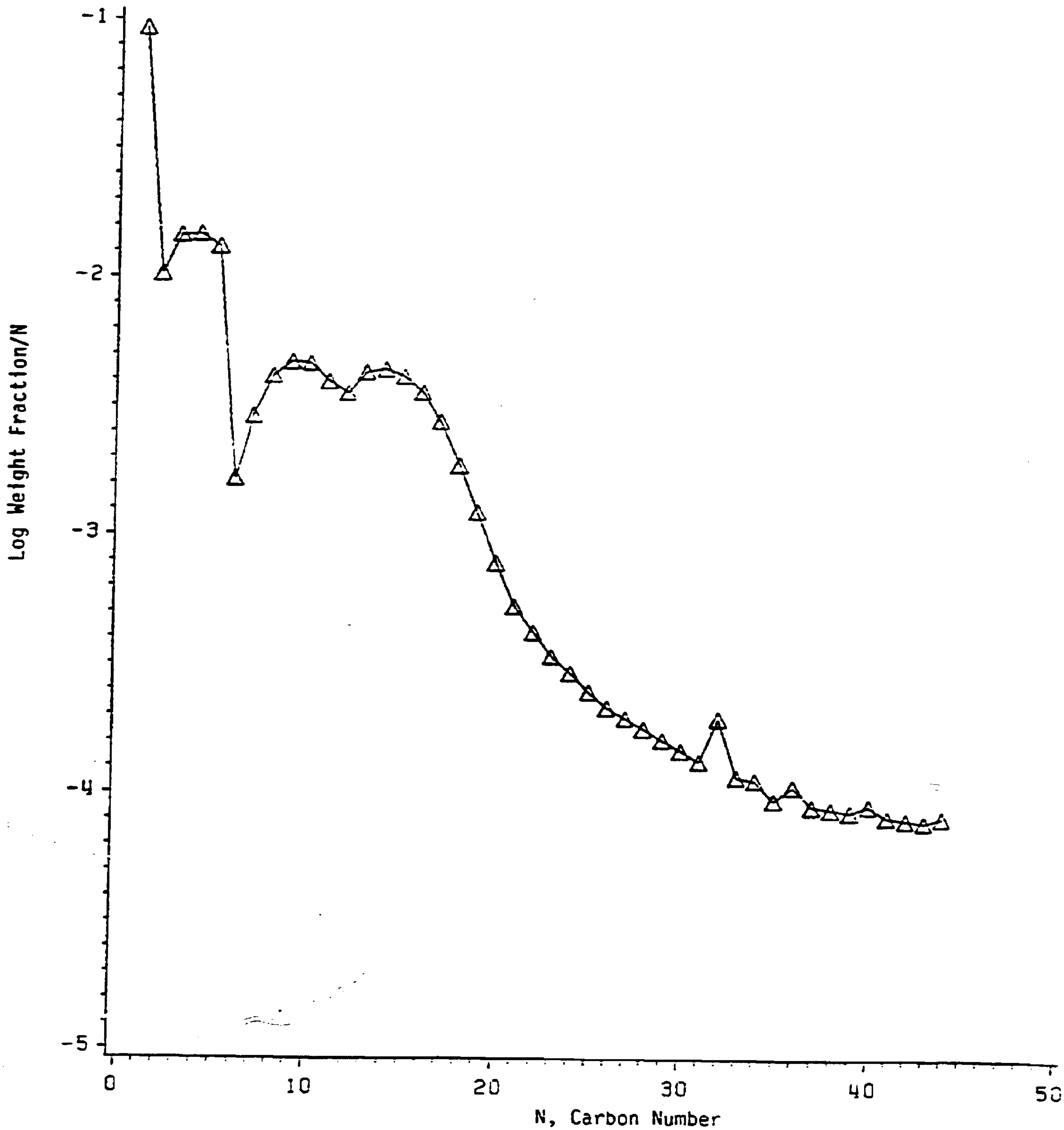

Figure 5-147. Anderson-Schulz-Flory Distributions with Catalyst 4966-76 with ≤2-4 nm Ruthenium in Run 19 (Hydrocarbons Only)

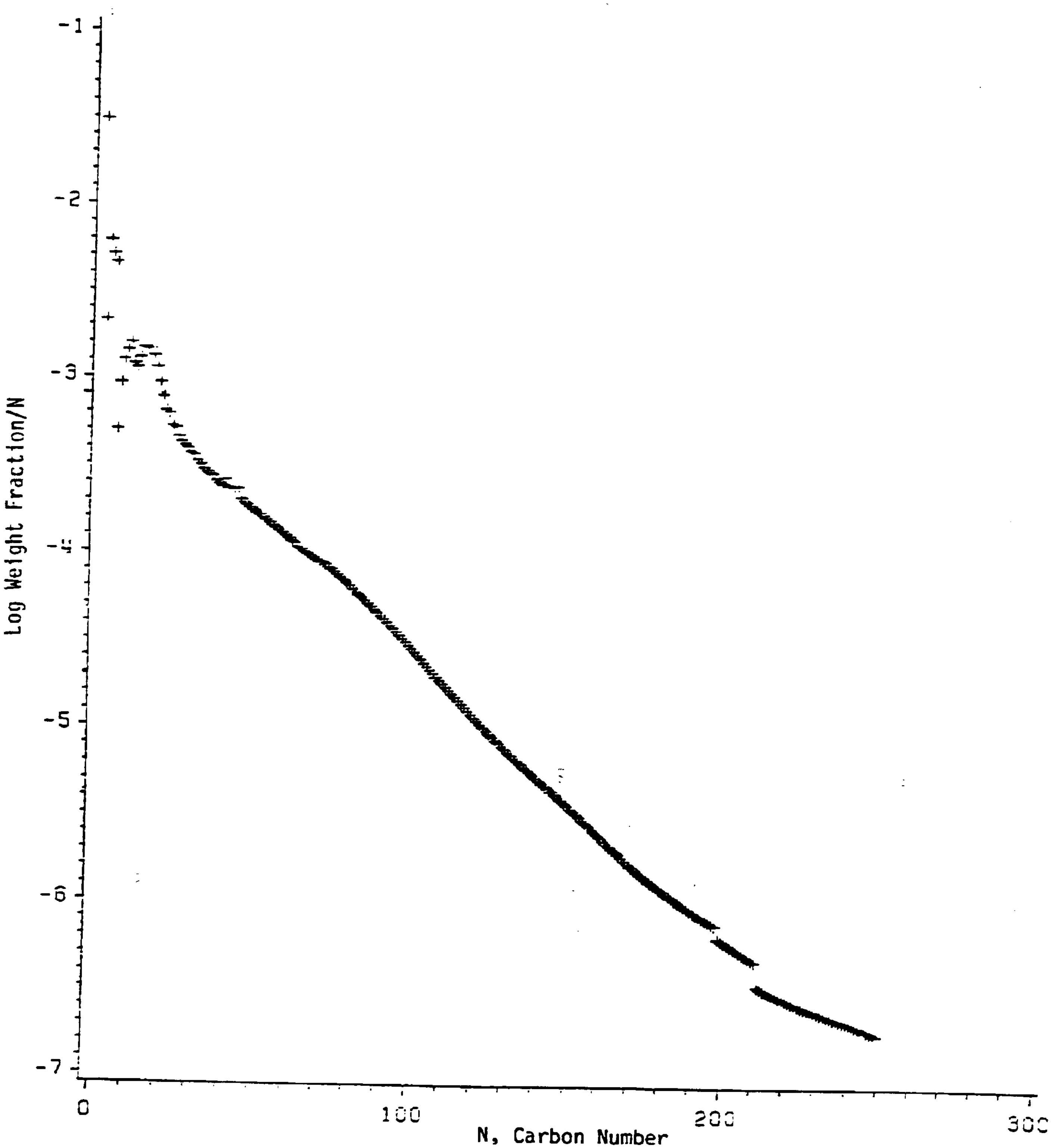

The initial CO conversion was 28% and gradually decreased to 4% by the end of the 100 hour-test (Figure 5-141). The CO selectivity to CO_2 decreased rapidly during the first 8 hours, and was nil during the test of the run (Figure 5-142). The H_2:CO usage ratio was about 2 after 8 hours on stream, confirming the absence of water gas shift activity (Figure 5-142).

Analysis of the inlet and outlet portions of Catalyst 4966-76 after the 100-hour-test showed much less ruthenium, 0.68% (by wt.), relative to 0.86% Ru in the fresh catalyst. Approximately half of the alumina particles that were examined from the catalyst inlet portion showed agglomerated ruthenium particles in 4-6 nm size range. The ruthenium on the remaining alumina particles apparently retained its original size. The number of alumina particles with agglomerated ruthenium was 50% less for the outlet portion relative to the catalyst at the inlet.

5.2.1.2.3 <u>Test at 1.5 H_2:CO Feed Ratio, 200°C at Inlet and 14.3 atm</u>

Catalyst 4966-76 with $\leq$2-4 nm ruthenium particles on γ-Al_2O_3 was tested at 1.5 H_2:CO feed ratio, 200°C and 14.3 atm for 12 hours in Run 20 (Tables 5-28 and 5-29 and Figures 5-148 through 5-151). Hydrocarbon cutoff at C_{11} was previously reported under these conditions with 4 nm size ruthenium particles encaged in Y-zeolite. The test in Run 20 was kept short in order to analyze products obtained prior to substantial ruthenium agglomeration.

The CO conversion increased from 12% to 20% during the test although the gas hourly space velocity was kept constant at 50 hr^{-1} (Figure 5-148). The CO selectivity to CO_2 was 33%-42%, while the H_2:CO usage ratio was 0.4% to 0.9%, apparently indicating substantial water gas shift activity. The ratio of olefinic to paraffinic products was 0 at carbon numbers 3 and 4.

Table 5-28. Product Distributions in Run 20

TOTAL PRODUCT DISTRIBUTION	
WEIGHT PCTS WITHOUT ARGON	
HYDROGEN	8.667
CARBON MONOXIDE	73.347
CARBON DIOXIDE	8.659
WATER	4.680
HYDROCARBONS	4.741
OXYGENATES	0.007
HYDROCARBON DISTRIBUTION	
C1	1.566
C2 - C4	2.655
C5 - C11	3.040
C12 - C18	0.779
C19 - C25	9.634
C26 PLUS	82.327
C1 - C44	30.457
C45 PLUS	69.543
OXYGENATES DISTRIBUTION	
ALCOHOLS	50.000
ALDEHYDES	50.000
OTHER OXYGENATES	0.000
MOLE PCTS WITHOUT ARGON	
HYDROGEN	58.202
CARBON MONOXIDE	35.449
CARBON DIOXIDE	2.633
WATER	3.517
HYDROCARBONS	0.198
OXYGENATES	0.001
RECOVERIES	
OVERALL	80.492
CARBON	78.835
HYDROGEN	82.493
OXYGEN	81.790
ARGON	79.189

GAS ANALYSIS, WT%	
HYDROGEN	8.6674
CARBON MONOXIDE	73.3466
CARBON DIOXIDE	8.5586
METHANE	0.0742
ETHANE	0.0146
ETHYLENE	0.0002
PROPANE	0.0403
PROPYLENE	0.0020
BUTANE	0.0407
BUTENE	0.0034
AQUEOUS ANALYSIS, WT%	
WATER	4.6800
ALCOHOLS	
C1	0.0000
C2	0.0000
C3	0.0000
C4	0.0017
C5	0.0017
C6	0.0000
C7	0.0000
C8	0.0000
C9	0.0000
C10	0.0000
ALDEHYDES	
C1	0.0000
C2	0.0000
C3	0.0000
C4	0.0000
C5	0.0017
C6	0.0017
C7	0.0000
C8	0.0000
C9	0.0000
C10	0.0000
OTHER OXYGENATES	
C1	0.0000
C2	0.0000
C3	0.0000
C4	0.0000
C5	0.0000
C6	0.0000
C7	0.0000
C8	0.0000
C9	0.0000
C10	0.0000

Table 5-29. Hydrocarbon Distributions in Run 20

C1	1.5657	C51	1.0055	C101	0.5091	C151	0.2107	C201	0.0769
C2	0.3123	C52	0.9952	C102	0.5012	C152	0.2064	C202	0.0752
C3	0.8933	C53	0.9849	C103	0.4933	C153	0.2023	C203	0.0736
C4	1.4493	C54	0.9747	C104	0.4854	C154	0.1982	C204	0.0720
C5	0.8433	C55	0.9646	C105	0.4776	C155	0.1942	C205	0.0704
C6	0.7419	C56	0.9410	C106	0.4698	C156	0.1902	C206	0.0688
C7	0.5536	C57	0.9310	C107	0.4621	C157	0.1864	C207	0.0673
C8	0.4322	C58	0.9211	C108	0.4545	C158	0.1826	C208	0.0658
C9	0.2952	C59	0.9112	C109	0.4469	C159	0.1788	C209	0.0643
C10	0.0975	C60	0.9013	C110	0.4394	C160	0.1751	C210	0.0629
C11	0.0758	C61	0.8915	C111	0.4320	C161	0.1715	C211	0.0615
C12	0.0254	C62	0.8725	C112	0.4246	C162	0.1680	C212	0.0601
C13	0.0016	C63	0.8628	C113	0.4173	C163	0.1645	C213	0.0507
C14	0.0000	C64	0.8531	C114	0.4109	C164	0.1611	C214	0.0574
C15	0.0000	C65	0.8434	C115	0.4038	C165	0.1578	C215	0.0560
C16	0.0000	C66	0.8337	C116	0.3967	C166	0.1545	C216	0.0547
C17	0.2534	C67	0.8241	C117	0.3898	C167	0.1513	C217	0.0535
C18	0.4984	C68	0.8145	C118	0.3829	C168	0.1481	C218	0.0522
C19	1.6465	C69	0.8050	C119	0.3761	C169	0.1450	C219	0.0510
C20	1.3505	C70	0.7827	C120	0.3694	C170	0.1420	C220	0.0498
C21	1.1397	C71	0.7733	C121	0.3627	C171	0.1424	C221	0.0487
C22	1.4794	C72	0.7639	C122	0.3562	C172	0.1395	C222	0.0475
C23	1.2513	C73	0.7545	C123	0.3497	C173	0.1367	C223	0.0464
C24	1.8086	C74	0.7452	C124	0.3433	C174	0.1339	C224	0.0453
C25	0.9579	C75	0.7359	C125	0.3370	C175	0.1312	C225	0.0442
C26	0.7725	C76	0.7267	C126	0.3308	C176	0.1285	C226	0.0432
C27	0.7746	C77	0.7174	C127	0.3246	C177	0.1259	C227	0.0421
C28	0.7843	C78	0.7044	C128	0.3186	C178	0.1233	C228	0.0411
C29	0.8228	C79	0.6952	C129	0.3126	C179	0.1208	C229	0.0402
C30	1.1790	C80	0.6861	C130	0.3118	C180	0.1183	C230	0.0387
C31	0.8467	C81	0.6769	C131	0.3060	C181	0.1159	C231	0.0378
C32	0.7157	C82	0.6678	C132	0.3002	C182	0.1136	C232	0.0369
C33	0.6589	C83	0.6588	C133	0.2946	C183	0.1112	C233	0.0360
C34	0.6402	C84	0.6498	C134	0.2890	C184	0.1090	C234	0.0351
C35	0.6838	C85	0.6408	C135	0.2835	C185	0.1067	C235	0.0343
C36	0.7084	C86	0.6320	C136	0.2781	C186	0.1046	C236	0.0334
C37	0.6823	C87	0.6231	C137	0.2727	C187	0.1024	C237	0.0326
C38	0.5627	C88	0.6144	C138	0.2675	C188	0.1003	C238	0.0318
C39	0.5106	C89	0.5995	C139	0.2623	C189	0.0983	C239	0.0311
C40	0.4975	C90	0.5909	C140	0.2572	C190	0.0962	C240	0.0303
C41	0.5016	C91	0.5824	C141	0.2522	C191	0.0942	C241	0.0296
C42	0.5140	C92	0.5740	C142	0.2472	C192	0.0923	C242	0.0289
C43	0.4760	C93	0.5656	C143	0.2423	C193	0.0904	C243	0.0281
C44	0.4525	C94	0.5573	C144	0.2375	C194	0.0885	C244	0.0275
C45	1.0771	C95	0.5490	C145	0.2328	C195	0.0866	C245	0.0268
C46	1.0661	C96	0.5408	C146	0.2281	C196	0.0848	C246	0.0261
C47	1.0552	C97	0.5327	C147	0.2236	C197	0.0830	C247	0.0255
C48	1.0444	C98	0.5246	C148	0.2190	C198	0.0820	C248	0.0248
C49	1.0337	C99	0.5165	C149	0.2193	C199	0.0802	C249	0.0242
C50	1.0160	C100	0.5171	C150	0.2150	C200	0.0785	C250	0.0236

Figure 5-148. Catalyst 4966-76 with <2-4 nm Ruthenium Particles: Conversions in Run 20 (H_2:CO Feed Ratio = 1.5, 200°C at Inlet, 14 atm)

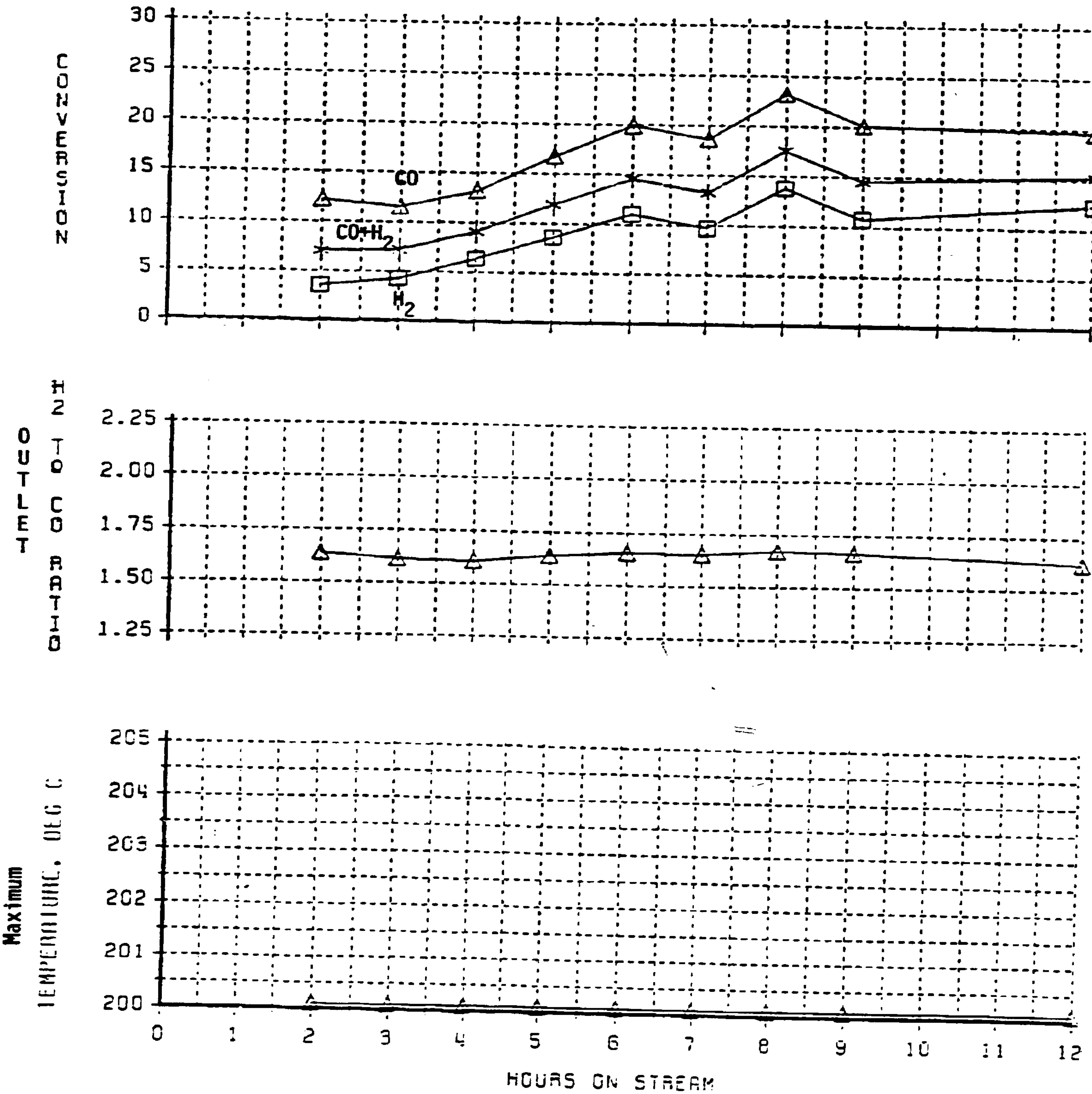

Figure 5-149. Catalyst 4966-76 with <2-4 nm Ruthenium Particles: Water Gas Shift Activity in Run 20 (H_2:CO Feed Ratio = 1.5, 200°C at Inlet 14 atm)

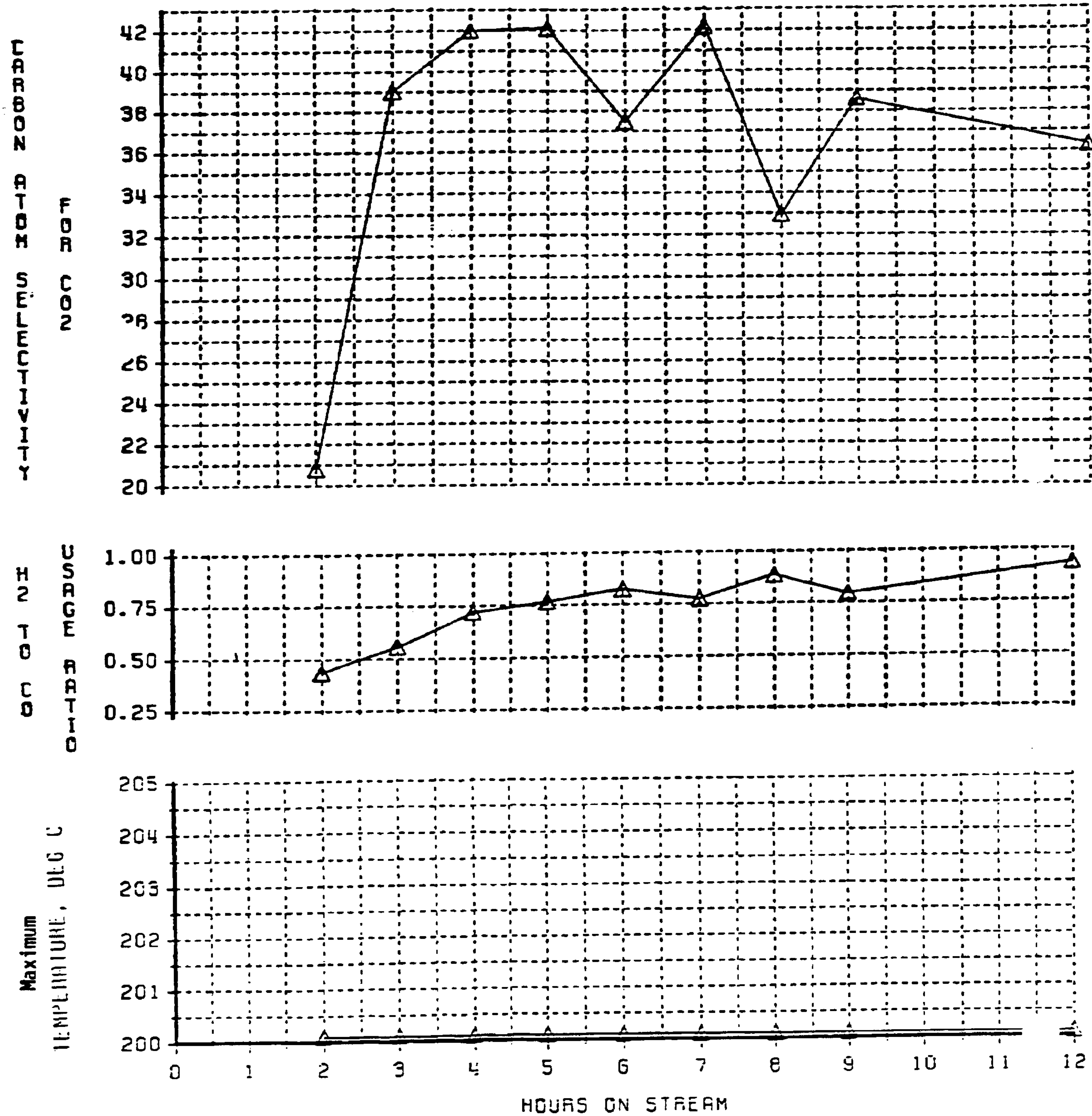

Figure 5-150. Catalyst 4966-76 with <2-4 nm Ruthenium Particles: C_1-C_4 Selectivities in Run 20 (H_2:CO Feed Ratio = 1.5, 200°C at Inlet, 14 atm)

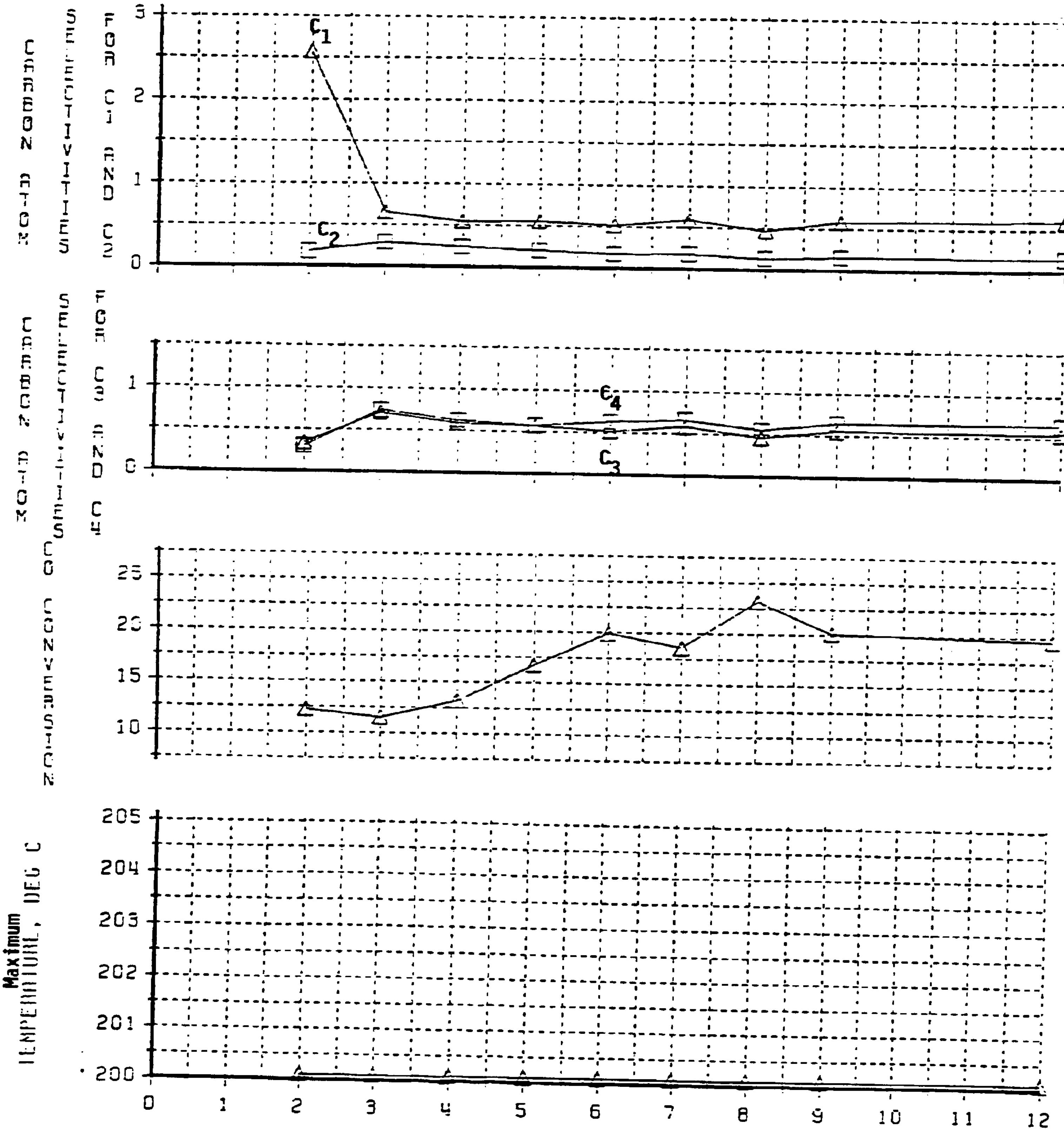

Figure 5-151. Anderson-Schulz-Flory Distribution with Catalyst 4966-76 Having ≤2-4 nm Ruthenium Particles in Run 20 (Hydrocarbons Only)

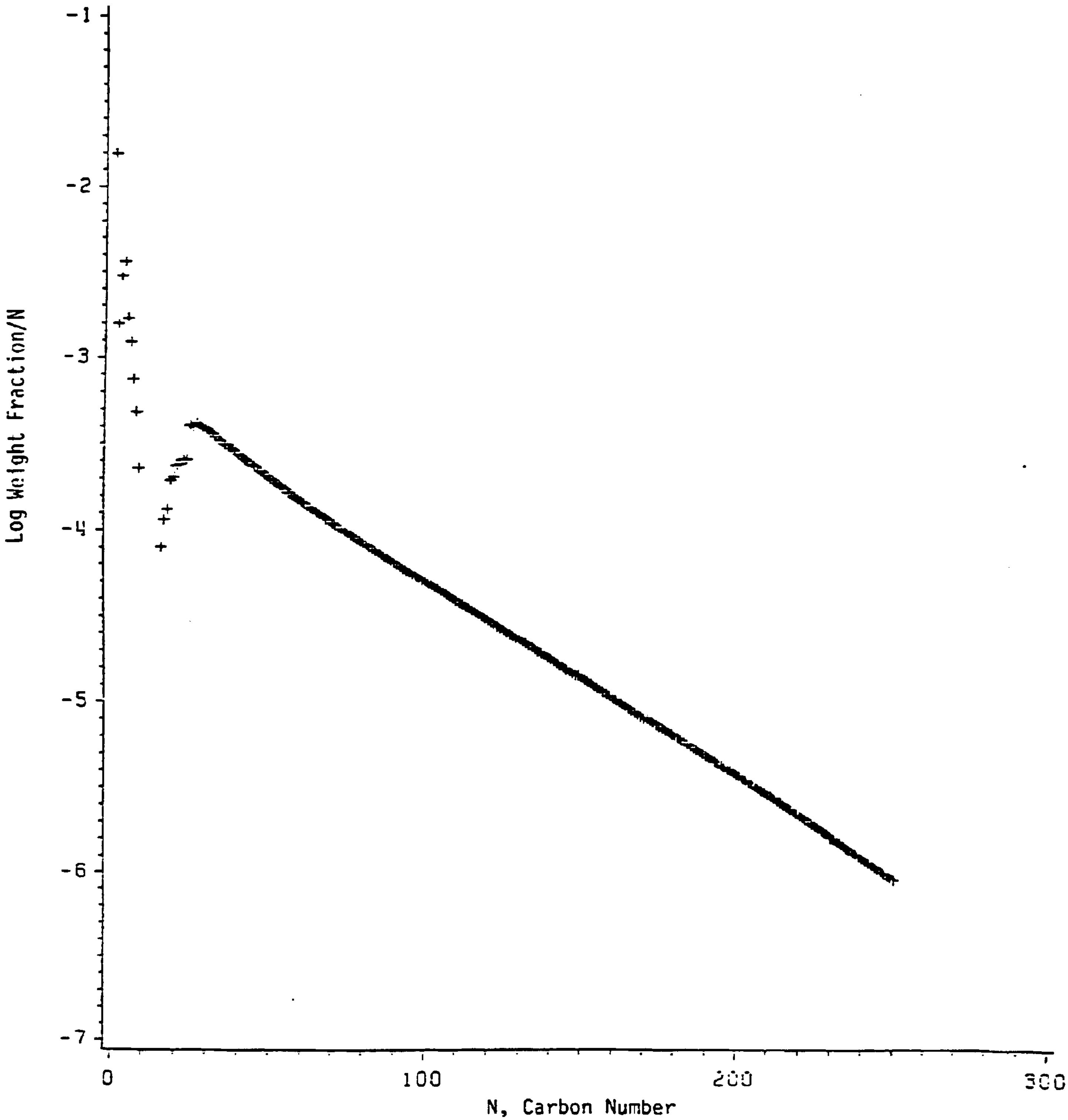

STEM analysis of the used catalyst indicated that, for 85% of the alumina particles, no noticeable ruthenium agglomeration had occurred. Approximately 15% of the examined alumina articles showed agglomerated ruthenium. The sizes of the agglomerated ruthenium particles were mostly 60-100 nm. These results indicate that, even if the specific activity of agglomerated ruthenium particles were high, the total exposed metal surface area by these agglomerated particles is too small to have catalytic significance. Therefore, products analyzed in Run 20 probably may be attributed to ruthenium particles which remained $\leq$2-4 nm during the run.

Gaseous products (C_1-C_5 hydrocarbons and CO_2) were accounted for by analyzing the effluent gas by GC. No significant amount of products were collected in the product receivers (one at 115° and 15 atm, the other at 0°C and 4 atm) during the course of the short test. The used catalyst underwent a soxhlet extraction with toluene for recovering the wax and was followed by a carbon burn measurement to determine the amount of coke on the used catalyst. The wax recovered from the used catalyst amounted to more than 83% (by wt.) of the hydrocarbons made (calculated based on the total CO converted) and showed an Anderson-Schulz-Flory distribution with $\alpha = 0.973$ up to a carbon number of 250 (Figure 5-151). The hydrocarbons that could not be recovered were in the C_5-C_{23} range and would normally be recovered in the product receivers in a long test. Nevertheless, since most products, particularly the heavy ones, were accurately analyzed, it was possible to conclude that hydrocarbon cutoff is not effected with $\leq$2-4 nm ruthenium particles supported on γ-Al_2O_3.

5.2.1.3 Catalysts with 3-500 nm Ruthenium Particles with ~1 Ru (by wt.)

A ruthenium catalyst (4956-23) unsuccessfully prepared on γ-alumina by a micelle method showed a broad size distribution of ruthenium particles between 4 to 500 nm (mostly 100-500 nm) in the STEM examination. This catalyst was nevertheless tested early in the program in the fixed-bed pilot plant in Run 9 to determine the catalytic activity and stability. The operating conditions were: 207°C inlet temperature, 103 atm, H_2:CO feed ratio = 0.9, 75 hr^{-1} GHSV, 81 hours. A stainless steel reactor was used. The results are described in Figure 5-152. The CO conversion decreased rapidly during the run from 43% to 10% in ~30 hours and then to 6% by the end of 81 hours.

Some of the products in Run 9 were also analyzed by GC/MS and IR and were found to contain iron and ruthenium carbonyls. The amounts of iron and ruthenium in the liquid products were determined by Atomic Absorption Spectroscopy (AAS) to be 0.41g and 0.0068g, respectively. AAS analysis done on the used catalyst indicated that there was no substantial ruthenium loss from the catalyst, while there was about 0.35 wt.% iron. Also, about 5% coke was analyzed on the used catalyst.

In an attempt to determine the causes of the rapid deactivation of Catalyst 4956-23, four more runs (Runs 11-14) were conducted with Catalysts 4956-27, 4956-30, 4956-22 and 4956-56, respectively. The micelle technique was not successfully applied to either of these four catalysts, which showed very broad size distributions of ruthenium particles in the range 3-500 nm (mostly 100-500 nm).

The CO conversions obtained in these runs are also summarized in Figure 5-152. Run 11 was conducted with an iron carbonyl scrubber held at 210°C on the CO/Ar feed line at the inlet of the reactor. Also, the operational pressure

Figure 5-152. Ruthenium Catalysts with Different Particle Size Distributions: CO Conversions *vs.* Time

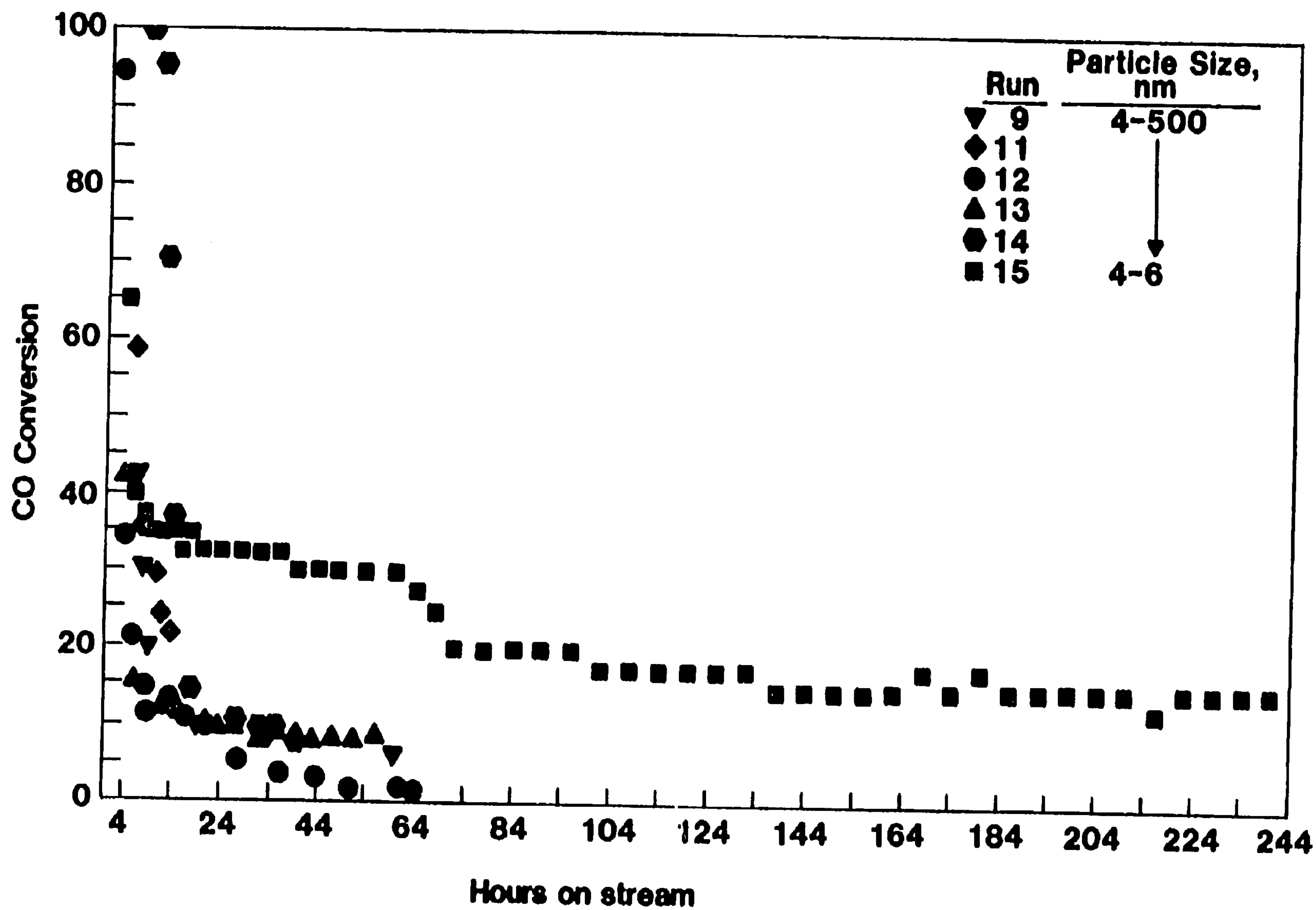

was lowered from 103 atm to 35 atm in order to minimize migration of ruthenium in the catalyst. The amount of iron on the catalyst in Run 11 was not lower than that observed in Run 9; however, the amounts of iron and ruthenium in liquid products were significantly lower. The same rapid deactivation was observed in Run 11 as in Run 9.

In Run 12, the temperature of the iron carbonyl scrubber was increased to 260°C. Less iron was analyzed both on the used catalyst and in the liquid products. However, catalytic stability was not apparently affected.

A glass-lined reactor was, for the first time, used in Run 13 in addition to the iron carbonyl scrubber at the reactor inlet to minimize contamination of the catalyst with iron. Very little iron was analyzed on the catalyst and in liquid products. However, catalytic stability was still poor.

Since relatively high coke levels, 5-7 wt.%, were analyzed on used catalysts in Runs 9 and 11-13, a higher H_2:CO feed ratio was used in Run 14 in order to minimize coking. The coke level in Run 14 was significantly lowered; however, the catalyst showed the same deactivation.

5.2.1.4 Catalysts with ~5 nm Average Size Ruthenium Particles with ~1% Ru (by wt.)

Tests with highly dispersed ruthenium catalysts and with ruthenium catalysts having ≤2-4 nm ruthenium particles indicated that catalytic activity and selectivity were influenced by ruthenium metal particle size on alumina. Also, catalysts with mostly very large ruthenium particles (100-500 nm) were unstable. In order to further investigate ruthenium metal particle size effects, catalysts with ~5 nm ruthenium particles were tested.